

Electric-field domain formation in type-II superlattices

H. Mimura, M. Hosoda, N. Ohtani, K. Tominaga, K. Fujita, and T. Watanabe

ATR Optical and Radio Communications Research Laboratories, Hikaridai Seika-cho, Soraku-gun, Kyoto 619-02, Japan

H. T. Grahn*

Research Center for Quantum Effect Electronics, Tokyo Institute of Technology, 2-12-1 O-okayama, Meguro-ku, Tokyo 152, Japan

K. Fujiwara

Department of Electrical Engineering, Kyushu Institute of Technology, Tobata-ku, Kitakyushu-shi 804, Japan

(Received 22 February 1996; revised manuscript received 15 April 1996)

Static electric-field domains as well as current self-oscillations due to domain-wall oscillations have been observed in undoped, type-II GaAs-AlAs superlattices under photoexcitation. Photoluminescence measurements clearly demonstrate the coexistence of low- and high-field domains in the static and oscillating domain voltage regime. A comparison with the calculated energy level distribution indicates that the static domains are connected with negative differential velocity (NDV) due to resonant transfer between X_2 in the AlAs layer and Γ_1 in the GaAs layer, while the oscillating domains are attributed to NDV originating from resonant tunneling between X_1 and X_2 in the AlAs layers. This observation demonstrates the importance of transport channels due to the indirect band structure of type-II superlattices. [S0163-1829(96)51328-7]

GaAs-AlAs short-period superlattices (SL's) have been intensively studied in recent years because their band structure can be of type-II.^{1,2} For certain values of the GaAs and AlAs layer thickness, the lowest-energy state in the conduction band occurs at the X_z minimum in AlAs and not at the Γ minimum in GaAs.³ For such a SL the application of an electric field should result in tunneling resonances between different X subbands as well as between X and Γ . Recently, it was demonstrated that Γ - X transport can drastically influence the carrier transport in type-I SL's.^{4,5}

In weakly coupled, type-I SL's, resonant tunneling in the conduction band usually occurs between different Γ subbands. For small carrier densities, the electric-field distribution across the superlattice is homogeneous. However, for intermediate and large carrier densities, the formation of stable and oscillating electric-field domains has been reported.⁶⁻¹² For stable domain formation, the electric field across the superlattice breaks up into two domains (a low-field domain and a high-field domain) with different field strengths corresponding approximately to the resonance condition.^{13,14} This phenomenon is due to the negative differential velocity (NDV) arising from resonant tunneling between different subbands in adjacent wells. Stable and unstable electric-field domains have also been investigated theoretically,¹⁵⁻¹⁷ supporting the interpretation of the experimental observations.

In this paper, we demonstrate that resonant tunneling between X subbands in the AlAs barrier of undoped type-II GaAs-AlAs SL's can also result in domain formation. Under photoexcitation stable domain formation as well as undamped oscillations of the current are observed. This is in strong contrast to undoped type-I SL's, in which, in addition to stable domains, so far only damped oscillations were observed.¹⁸ The origin of the domain formation in type-II SL's is attributed to resonant tunneling between X subbands

as well as X - Γ transfer effects, because the resonance field strengths can be directly obtained from photoluminescence measurements.

The SL is embedded in an n - i - n structure, which is grown on a (100)-oriented n^+ -type GaAs substrate by molecular-beam epitaxy (MBE). It consists of an n^+ -GaAs buffer layer (0.2 μm , $2 \times 10^{18} \text{ cm}^{-3}$ Si-doped), an n^+ -Al_{0.4}Ga_{0.6}As cladding layer (0.2 μm , $5 \times 10^{17} \text{ cm}^{-3}$ Si-doped), the intrinsic layer containing the SL, an n^+ -Al_{0.4}Ga_{0.6}As cladding layer (0.2 μm , $5 \times 10^{17} \text{ cm}^{-3}$ Si-doped), and an n^+ -GaAs cap layer (50 nm, $2 \times 10^{18} \text{ cm}^{-3}$ Si-doped). The intrinsic region contains a 75-period, undoped GaAs-AlAs SL with nominally 3.4 nm GaAs and 5.1 nm AlAs layer thickness. The sample is processed into 50 μm square mesas with alloyed Au electrodes as contacts. A cw He-Ne laser at 632.8 nm is used to vary the carrier density in the SL. The laser beam is focused onto the n^+ -GaAs cap layer of the sample, which is mounted in a closed-cycle cryostat, through a microscope objective with a beam diameter of about 20 μm . We used a semiconductor parameter analyzer (YHP 4145B), a sampling oscilloscope (Tektronix 7854), a spectrum analyzer (HP 8566B), and a streak camera (Hamamatsu C4334) for the current-voltage (I - V), time-resolved current, oscillation frequency spectra, and photoluminescence (PL) measurements, respectively. The photocurrent (PC) spectra are also measured to determine the absorption edge of the SL.

The superlattice is designed to be of type-II, i.e., the X_{z1} and X_{z2} levels in AlAs are below the Γ_1 level in GaAs. The energy band structure of the conduction is shown schematically in Fig. 1(a). The I - V characteristics at 20 K in the dark and under photoexcitation of 1 mW are shown in Fig. 2. The positive sign of the bias voltage corresponds to the condition of applying a positive bias to the substrate contact. While the dark characteristic is almost symmetric and does not exhibit

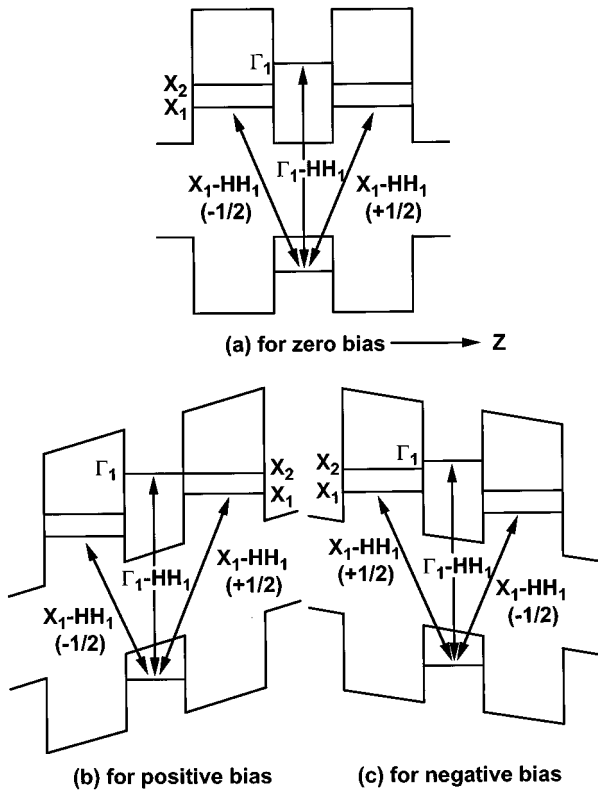


FIG. 1. Schematic diagram of the energy level structure in the conduction band of the investigated type-II GaAs-AlAs superlattice (a) at zero bias, (b) at positive bias for resonant transfer from X_2 to Γ_1 , and (c) at negative bias for resonant tunneling from X_1 to X_2 .

any sign of domain formation (between -8 and 8 V the dark current is below 1 pA), the characteristic under photoexcitation clearly shows the signature of domain formation. Between 4 and 10 V, a ratchetlike structure emerges, which is typical for stable electric-field domain formation. However, for negative voltages, this ratchetlike structure does not appear for this excitation intensity, although clear plateaus are visible between -1.7 and -4.8 V as well as between

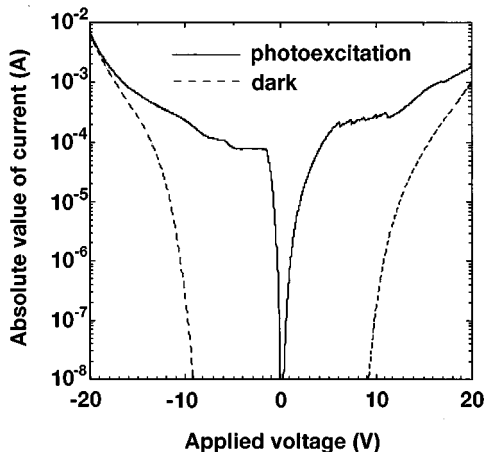


FIG. 2. I - V characteristics in the dark and for a laser intensity of 1 mW at 20 K. A positive voltage corresponds to a positive bias applied to the n^+ -GaAs substrate.

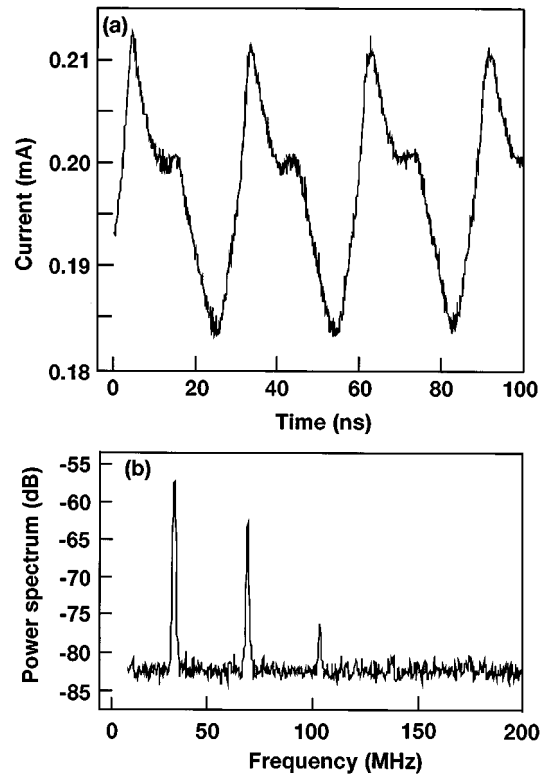


FIG. 3. Time-resolved photocurrent at -3 V (a) and corresponding power spectrum (b) at 20 K for a laser intensity of 2.5 mW.

-5.5 and -7.5 V. This plateaulike I - V characteristic without any fine structure is indicative for oscillating domains.^{11,12} Similar I - V characteristics are obtained for intensities between 0.15 and 8 mW. The onset voltage of the ratchetlike structures in the positive bias direction, however, decreases with decreasing laser intensity. No ratchetlike structures or plateau regions are observed for intensities below 50 μ W. The asymmetry of the I - V characteristics under photoexcitation with regard to the bias direction is attributed to the inhomogeneous absorption profile and carrier distribution, which results in an asymmetry of the current flow for different bias directions.

Self-oscillations of the photocurrent occurred for negative bias in the first plateau region for laser intensities between 0.5 and 8 mW. Figure 3 shows the time-resolved current at -3 V (a) and its power spectrum (b) measured simultaneously with a spectrum analyzer for an intensity of 2.5 mW at 20 K. The oscillations are not purely sinusoidal, but contain higher harmonics. In the positive bias direction oscillations are only detected for intensities above 10 mW. However, these oscillations appear in a different bias range (between 15 and 20 V) and exhibit higher frequencies (fundamental frequency is 150 MHz). They are also present for negative bias in the same voltage and intensity range.

To determine the origin of domain formation in this type-II SL, PL spectra have been recorded. We also measured PC spectra to determine the direct energy gap of the SL. In Fig. 4 the PL spectra are shown for positive bias. The spectra were recorded at 20 K for a laser intensity of 1 mW. The dominant PL bands are shown schematically on the

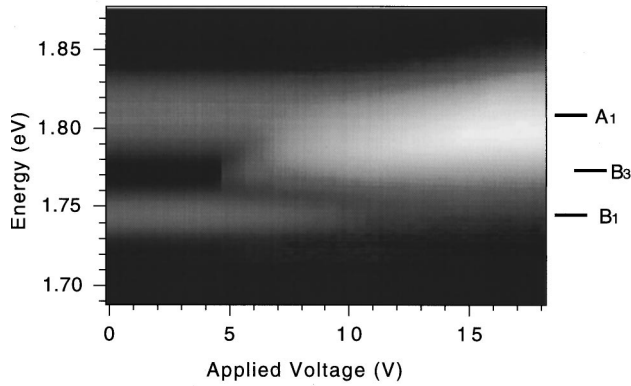


FIG. 4. PL spectra as a function of the positive bias at 20 K for a laser intensity of 1 mW. The PL intensity is indicated on a gray scale, where a large intensity corresponds to a bright region.

right-hand side of the figure. At zero field there are two PL bands, one at 1.746 eV (B_1) and a second one at 1.810 eV (A_1). Comparing these energies with the PC spectra the peak A_1 clearly originates from recombination of Γ_1 electrons in the GaAs wells with heavy holes HH_1 . The peak B_1 is then identified as the indirect recombination from X_1 electrons in the AlAs barriers with HH_1 . In the voltage range of static domain formation between 6 and 11 V (cf. Fig. 2), three coexisting PL lines can be clearly identified. In addition to the two lines at zero voltage (A_1 and B_1), which do not change their energy, the new line appears energetically between the previous two at 1.771 eV (B_3). The coexistence and constant energy of these lines in this voltage range clearly support the interpretation of domain formation.^{13,14} In an applied electric field the direct PL line from Γ electrons should display a redshift due to the Stark effect, which becomes negligible for very narrow quantum wells. However, the indirect PL line from X electrons, which at zero field [cf. Fig. 1(a)] actually originates from two energetically degenerate states $X_1(-1/2)$ and $X_1(+1/2)$, splits into two lines. For a positive electric field F , the first one is redshifted by $-eFd/2$, while the second one is blueshifted by $eFd/2$, where d denotes the SL period. This energy shift is typical for indirect gap SL's,¹⁹ and it has been previously observed in PL spectra^{20,21} and electroreflectance spectra.²² The blueshifted line has the larger intensity, since in an electric field the overlap between the electron and hole wave functions is larger for this field direction. We therefore attribute B_3 to the blueshifted X_1 - HH_1 recombination. The blueshift of the X_1 - HH_1 line is 25 meV, which corresponds to an electric-field strength of 59 kV cm⁻¹. The redshift of A_1 is too small to be observed, since the quantum well is very narrow.

Using an envelope function calculation of the Kronig-Penney model, the separation between X_1 and X_2 is determined to be 30 meV, corresponding to a resonance field strength of 35 kV cm⁻¹ ($X_2 - X_1 = eFd$). We assumed a quantum-well width of 2.8 nm to reproduce the observed direct energy gap of the SL. The energy difference between X_2 and Γ_1 is 29 meV, resulting in a field strength for resonant transfer of 68 kV cm⁻¹. In this case the centers of the wave functions are only separated by $d/2$ so that $X_2 - \Gamma_1 = eFd/2$ [cf. Fig. 1(b)]. The PL line B_3 therefore

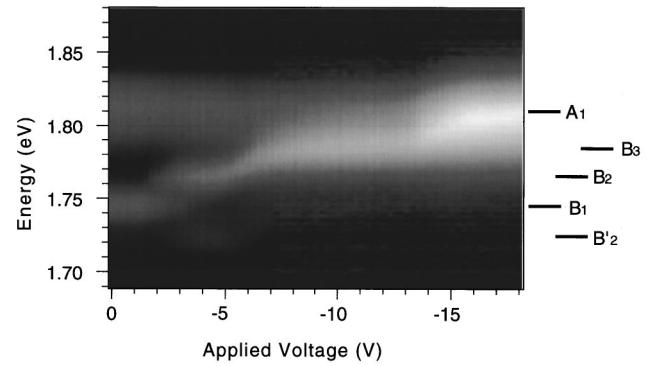


FIG. 5. PL spectra as a function of the negative bias at 20 K for a laser intensity of 1 mW. The PL intensity is indicated on a gray scale, where a large intensity corresponds to a bright region.

originates from a spatial region, which corresponds to a high-field domain due to resonant transfer of carriers between X_2 and Γ_1 as shown in Fig. 1(b). The complete tunneling process covers two periods, nonresonant tunneling from X_1 to X_2 , followed by transfer to Γ_1 in the next well and transfer into X_2 in the next barrier. The field strength of the high-field domain is usually somewhat smaller than the corresponding resonance field strength.¹⁸

The I - V characteristic under photoexcitation (cf. Fig. 2) looks very different in the negative bias direction. A first plateau appears between -1.7 and -4.8 V. This is the region where the current self-oscillations are observed. A second, less pronounced plateau occurs between -5.5 and -7.5 V. In this voltage regime, no self-oscillations are observed. We again use PL spectroscopy to determine the field distribution in this bias direction. In Fig. 5 the PL spectra are shown for a laser intensity of 1 mW at 20 K. Since this PL spectrum contains several lines, the respective energies are indicated on the right-hand side of the figure. At zero field, we again observe two lines (A_1 and B_1) corresponding to the recombination from Γ_1 - HH_1 and X_1 - HH_1 . In the first plateau region, four PL lines are observed, A_1 and B_1 as well as B_2 and B'_2 at energies 1.766 and 1.727 eV, respectively. These last two transitions originate from the blueshifted $X_1(+1/2)$ and redshifted $X_1(-1/2)$ state. The corresponding field strength is the same for both lines with a value of about 47 kV cm⁻¹, which is closer to the $X_1 \rightarrow X_2$ tunneling resonance [cf. Fig. 1(c)] than to the $X_2 \rightarrow \Gamma_1$ resonant transfer field strength [cf. Fig. 1(b)]. Therefore, in the low-field domain electrons tunnel resonantly from X_1 to X_1 in adjacent wells, while in the high-field domain resonant tunneling occurs between X_1 and X_2 . Between -5 and -6.5 V line B_2 shifts linearly to higher energies, while B_1 and B'_2 have disappeared. This shift occurs in the voltage range, where the current strongly increases from the first to the second plateau (cf. Fig. 2). The field is assumed to be homogeneously distributed in this voltage range. Below -6.5 V, the PL line remains constant in energy at 1.784 eV. Within the second plateau we expect a coexistence of field strengths corresponding to $X_1 \rightarrow X_2$ tunneling resonance [cf. Fig. 1(c)] and $X_2 \rightarrow \Gamma_1$ resonant transfer [cf. Fig. 1(b)]. We therefore identify the PL line at 1.784 eV as B_3 , although it occurs at somewhat higher energies than for positive bias. It remains at this energy even for voltages much beyond the end of the

second plateau in the I - V characteristics. However, it is possible that a tunneling resonance in the valence band between HH1 and light-hole ground state LH₁ is masking the resonance between X_2 and Γ_1 . For voltages below -13 V, the PL line B_3 appears to shift to higher energies again until at -15 V it coincides with A_1 . Assuming again a linear Stark shift for spatially indirect transitions with one half of the SL period, the electric field is estimated to be 150 kV cm⁻¹, which agrees quite well with the field strength for resonant transfer from X_1 into Γ_1 . However, no plateau-like structure is observed in the I - V characteristics in this field range. The strong asymmetry between positive and negative bias under photoexcitation can be explained by a hole accumulation near the top contact, when a positive bias is applied. This accumulation does not occur for the negative bias direction, since holes are photoexcited near the top contact, but move towards the bottom contact.

In summary, electric-field domain formation has been

observed in undoped type-II GaAs-AlAs superlattices under photoexcitation. Static domains as well as oscillating domains are identified. Photoluminescence spectra are used to determine the involved tunneling resonances. The static domains for positive bias are due to NDV originating from resonant transfer between X_2 in AlAs and Γ_1 in GaAs, while the oscillating regime for negative bias occurs due to a coexistence of $X_1 \rightarrow X_1$ and $X_1 \rightarrow X_2$ resonances in the AlAs layers. This observation clearly demonstrates the importance of X -state tunneling resonances and $X \rightarrow \Gamma$ resonant transfer in type-II superlattices in an applied electric field.

The authors would like to thank M. Nakayama (Osaka City University) for stimulating discussions and H. Inomata and E. Ogawa for their constant encouragement. One of us (H.T.G.) would like to thank ATR Optical and Radio Communications Research Laboratories for their hospitality.

*Permanent address: Paul-Drude-Institut für Festkörperelektronik, Hausvogteiplatz 5-7, D-10117 Berlin, Germany.

¹J. Feldmann *et al.*, Phys. Rev. B **42**, 5809 (1990).

²M. Nakayama, K. Suyama, and H. Nishimura, Phys. Rev. B **51**, 7870 (1995).

³M. Nakayama, I. Tanaka, I. Kimura, and H. Nishimura, Jpn. J. Appl. Phys. **29**, 41 (1990).

⁴H. Mimura *et al.*, Appl. Phys. Lett. **67**, 3292 (1995).

⁵M. Hosoda *et al.*, Phys. Rev. Lett. **75**, 4500 (1995).

⁶L. Esaki and L. L. Chang, Phys. Rev. Lett. **33**, 495 (1974).

⁷K. K. Choi, B. F. Levine, R. Malik, J. Walker, and C. G. Bethea, Phys. Rev. B **35**, 4172 (1987).

⁸H. T. Grahn, R. J. Haug, W. Müller, and K. Ploog, Phys. Rev. Lett. **67**, 1618 (1991).

⁹J. Kastrup *et al.*, Appl. Phys. Lett. **65**, 1808 (1994).

¹⁰S. H. Kwok *et al.*, Phys. Rev. B **51**, 10 171 (1995).

¹¹H. T. Grahn *et al.*, Jpn. J. Appl. Phys. **34**, 4526 (1995).

¹²J. Kastrup *et al.*, Phys. Rev. B **52**, 13 761 (1995).

¹³H. T. Grahn, H. Schneider, and K. v. Klitzing, Appl. Phys. Lett. **54**, 1757 (1989).

¹⁴H. T. Grahn, H. Schneider, and K. v. Klitzing, Phys. Rev. B **41**, 2890 (1990).

¹⁵B. Laikhtman and D. Miller, Phys. Rev. B **48**, 5395 (1993).

¹⁶L. L. Bonilla, J. Galán, J. A. Cuesta, F. C. Martinez, and J. M. Molera, Phys. Rev. B **50**, 8644 (1994).

¹⁷F. Prengel, A. Wacker, and E. Schöll, Phys. Rev. B **50**, 1705 (1994).

¹⁸S. H. Kwok *et al.*, Phys. Rev. B **51**, 9943 (1995).

¹⁹D. M. Whittaker, M. S. Skolnick, G. W. Smith, and C. R. Whitehouse, Phys. Rev. B **42**, 3592 (1990).

²⁰M.-H. Meynadier *et al.*, Phys. Rev. Lett. **60**, 1338 (1988).

²¹D. M. Whittaker, M. S. Skolnick, G. W. Smith, and C. R. Whitehouse, Phys. Rev. B **42**, 1990 (3591).

²²A. J. Shields, P. C. Klipstein, M. S. Skolnick, G. W. Smith, and C. R. Whitehouse, Phys. Rev. B **42**, 5879 (1990).